Díaz-Álvarez, A., Rodríguez-Millán, M., Díaz-Álvarez, J., y Miguélez, M.H. (2018). Experimental analysis of drilling induced damage in aramid composites, *Composite Structures*, 202, pp. 1136-1144.

DOI: https://doi.org/10.1016/j.compstruct.2018.05.068

Funding: Ministry of Economy and Competitiveness of Spain and FEDER program under the Projects: RTC-2015-3887-8, DPI2017-88166-R and DPI2017-89197-C2-1-R

Experimental analysis of drilling induced damage in aramid composites

A. Díaz-Álvarez[a,*], M. Rodríguez-Millán[a], J. Díaz-Álvarez[b], M.H. Miguélez[a]

[a] Department of Mechanical Engineering, University Carlos III of Madrid, Avda. de la Universidad 30, 28911 Leganés, Madrid, Spain
[b] Department of Aerospace Engineering, University Carlos III of Madrid, Avda. de la Universidad 30, 28911 Leganés, Madrid, Spain

A B S T R A C T

Aramid composites are increasingly used alone or combined with other composites in structural and personal protections due to the current demand of these applications against ballistic or fragment hazards. Drilling is a common operation required prior to mechanical joining of components, however this operation has been poorly analyzed in the case of aramid composites. Drilling induced damage of this family of composites is analyzed in the present work considering the effect of the drill geometry and cutting parameters. Fuzzing was the dominant damage mechanism both at hole entry and exit being also found delamination in most cases. Drill geometry and feed were influential parameters on resultant composite damage. Main contribution of this work is the ob-tainment of phenomenological expressions derived from experimental data, allowing the prediction of damage extension as a function of cutting parameters.

A R T I C L E I N F O

Keywords:
Aramid composites
Fabrics/textiles
Drilling induced damage

1. Introduction

Composites are usually made near net shape, however some machining operations are required to achieve final dimensional tolerance and joining requirements. Despite the advances of adhesive techniques [1] mechanical joining [2] is the common procedure requiring prior drilling of the hole.

Composites are considered as low machinability materials because of the trend to experience damage during drilling because of their nature, composed of two or more phases and the abrasive character of the fibers inducing rapid wear of the cutting tool [3]. The induced damage during drilling causes an elevated percentage of workpiece rejection in aerospace for instance [4] and is due to inadequate cutting parameters, erroneous drill geometries and excessive tool wear [5–8]. Although the problem of drilling induced damage is common for all families of composites, the damage mode and the most influencing parameters depend on the type of composite. For instance, delamination has been reported as the critical damage mechanism in CFRPs [9–13] while in the case of biodegradable composite materials, fraying is much more important [14,15].

Aramid composites are increasingly used due to low density, heat-resistant, high tensile strength, high hardness and resistance to corrosion and chemical agents [16]. This family of composites (mainly based in the commercial fiber Kevlar) is suitable for applications requiring elevated energy absorption capability in automotive, aeronautical [13,14] and naval industries [17] as well as military equipment and protection due to the rise of terrorism and international conflicts [18–20].

Drilling of aramid fiber composite is characterized by a poor surface finishing leaving uncut fibers on both sides of the drilling (enter and exit), where the predominant damage factor is fuzzing [21], and secondly delamination [22]. Fuzzing damage is mainly generated due to the plastic deformation and fibrillation generated from fiber fracture, characteristic of the ductile fiber with a structure oriented in the axial direction experiencing large elongation before fracture [21].

Proper drilling of aramid composite requires the use of suitable tool geometry and cutting conditions. In this sense, there is a lack of research in the drilling analysis of aramid composites, existing few recent works and some early publications studies in the 90 s dealing with this important topic.

Main contributions concerning the analysis of drilling of aramid composites are briefly summarized in the following paragraphs.

Bishop and Gindy [23] analyzed drilling of aramid composites with a phenolic polyvinylbutyral matrix of 4 mm thickness. Experimental tests were carried out with two drills; a High Speed Steel (HSS) twist drill with different point and helix angles and a HSS tube drill of 9.5 mm external diameter and a thickness of 1 mm, in order to establish a comparative between both drills and its influence on the hole damage. The tests were carried out at two different speeds and feeds (20 and 50 m/min and 0.05 mm/rev and 0.09 mm/rev respectively). They concluded that increments in point or rake angles lead to an improvement in hole quality. Thrust force was also found dependent of the point angle, showing a maximum at 180° and a reduction at angles greater than the value mentioned. Torque decreases with increments on

rake angle, but shows few changes with the variation of the point angle. The effect of cutting speed and feed on torque, thrust force and hole quality, were negligible when compared to the effects of tool geometry.

Di Ilio and collaborators [24,25] carried out drilling test in 3 mm aramid composite with sintered tungsten carbide drills (commercially available) of 3 mm diameter. The cutting speed was 120 m/min and the feed rate were varied from 0.006 and 0.07 mm per revolution. They found that the thrust force showed irregular courses which were discussed in terms of non-uniform distribution of the thrust force along the tool cutting edges and also because of the poor interlaminar strength in the composite. Likewise, they related a continuous decrease on the thrust force during drilling with a reduction of the material strength as a consequence of the temperature increase at the cutting front. Moreover, they studied the delamination through the thickness of the laminate.

Bhattacharyya and Horrigan [26] developed an investigation using two different HSS drills (10 mm diameter twist drill with 118° point angle and 12 mm twist drill with −20° point angle) in different environmental testing conditions (ambient and cryogenic temperatures). They found that cryogenic conditions caused an increment of the thrust force.

Shuaib et al. [27] carried out experimental tests in plain weave aramid composites with different thicknesses using a TiN coated twist drill (6 mm diameter). The machining parameters were a cutting speed of 23 and 57 m/min; and a feed of 0.025 and 0.1 mm/rev. They concluded that torque and thrust force tends to increase with increments in the cutting parameters and the composite thickness respectively. Furthermore, cutting parameters and the thickness of the aramid composite have significant influence on the quality of drilled holes.

Recently, Wu et al. [22] developed an experimental and numerical study of the residual stresses generated in a 3.5 mm aramid fiber composite using an interferometry technique. They found that the residual stress components of each specimen were compressive along the aramid yarns direction and tensile in the perpendicular direction. In addition, the authors analyzed the influence of the drill penetration through the composite on the residual stress and showed that residual stress decreased with increments in drill depth.

Sinan Liu et al. [28] studied the influence of the gap between a collar (whose function was to compress the Kevlar laminates during a drilling process) with the drill on different damages as: fuzzing area, delamination and tearing length.

Main contributions in the field are summarized in Table 1, illustrating drill geometry and cutting parameters of each work reviewed for clarity.

Despite the interest of drilling aramid composites this process has been poorly analyzed in the literature. This work focuses on the study of aramid composite drilling with especial attention to the damage induced in the workpiece. The influence of the drill geometry on the damage, thrust force and torque has been analyzed. Fuzzing was the main defect observed during drilling of the aramid composite being also found delamination in most of cases. The relation between cutting parameters and the quality of the final product was achieved through the development of mechanistic models. Reasonable accuracy was observed in the predictions of cutting forces and damage.

2. Experimental setup

2.1. Workpiece material

Aramid composite with areal density 8.86 kg/m^2 was analysed. It was provided in rectangular plates that were cut in samples of $200 \times 28 \times 3.5\,mm^3$ and consists of 12 layers of aramid fabric impregnated in phenolic matrix (Polyvinyl butyral phenolic) by manual stacking and then hot pressed. These dimensions were required in order to perform drilling operation confined inside a special device, allowing air entrance and connected to a vacuum, with the aim of collecting the dust fibres generated during chip removal. The composition of composite is commonly used by manufacturers and was used in [22] being main properties summarized in the Table 2.

2.2. Machine tool

The drilling tests were performed without coolant in a B500 KONDIA machining center instrumented with a dynamometer (Kistler 9123C) allowing the measurement of the thrust force with a range of −2 to 2 KN and the torque within a range of −20 to 20 Nm, Fig. 1.a).

A special device was developed to ensure a precise control of the position of the test specimen and a proper vacuum of the dust generated during the drilling process. On one hand, the specimen is clamped within two metallic plates (previously drilled with a hole with a diameter close to the nominal diameter) allowing a free delamination of the different layers (see detail Fig. 1.b)), it was used since a decrease of delamination damage has been reported in CFRP using this procedure [9]. On the other hand, the clamping system is sealed within a box connected to a pipe through which the dust is vacuumed.

2.3. Drill geometries and cutting parameters

Two different types of drill with nominal diameter equal to 6 mm and based on an uncoated CW (Tungsten carbide) substrate were tested (drills geometry is illustrated in Fig. 2):

- Drill-A: HSS twist drill with 118° point angle. This type of drill has been commonly used in the literature because of its moderate cost and quality [23–26].
- Drill-B: HSS brad & spur drill with 110° point angle (denoted). This type of drill has been by manufacturers and was used by Veniali et al. in previous works [24,25]

Cutting parameters were stated in the range recommend by manufacturers and commonly reported in the literature (see Table 1). Six different values of cutting speed (V, 23 m/min–110 m/min) and three values of feed rate (f, 0.025 mm/rev to 0.1 mm/rev), were analyzed (see Table 3).

2.4. Damage measurement

A stereo microscope (Optika SZR) has been used in order to estimate the damaged area in the drilled specimens. Main damage mode was fuzzing, finding delamination as complementary damage in most of the cases analyzed. Delamination can be observed in the workpiece (Fig. 3) through a bulging of the specimen surface both at the entrance and at the exit, which leads to an increase in the thickness of the sample in the influence area of the drill.

The parameter to quantify the damage in the workpiece (W_d, *workpiece damage*) is defined in terms of the maximum diameter of the damaged area, which include both fuzzing damage and delamination, D_{max} (*Maximum diameter at which delamination was found*), and the nominal diameter of the hole, D_{nom}, as suggested other authors, see for instance [25] (see Fig. 3):

$$W_d = \frac{D_{max}^{damage} - D_{nom}}{2} \quad (1)$$

The damage at the hole entry is due to pull out effect of the cutting edges of the drill bit causing the separation of the firsts layers. On the other hand, the push out effect of the tool in the last layers results in the generation of damage at the hole exit. Both damage at the hole entry and exit are related to the aramid fiber nature with high elongation before breakage causing: fuzzing due to uncut fibers around the hole, and delamination due to the edges of the drill in the first layers as well as the effect of the tool pushing on the last layers during drilling.

Table 1
Main cutting parameters and drills used in previous investigations. Nomenclature: t = thickness, Φ = Diameter of drill, f = feed, V_c = cutting velocity.

Drill geometry	References	Cutting parameters
Twist Drill [29] 	Bishop et al. [23]	t: 4 mm;Φ: 12.5 mm; f: 0.05–0.09 mm/rev; V_c: 19.4,50.5 m/min; Coating: without.
	Bhattacharyya et al. [26]	t: 6 mm;Φ: 10 mm;f: 0.1 mm/rev;V_c: 30 m/min; Coating: without.
	Sinan Liu et al. [28]	t: 3.5 mm;Φ: 6mm;fr: 20,40,80 mm/min; Coating: without.
	Shuaib et al. [27]	t: 2.4–16.4 mm; Φ: 6 mm;f: 0.1,0.025 mm/rev; V_c: 23–57 m/min; Coating: TiN.
	Mufarrih et al. [30] Won et al. [31]	t: 6 mm; Φ: 10 mm;f: 0.1–0.3 mm/rev; V_c: 47–79 m/min; Coating: without.
	Di Ilio et al. [24]	t: 8.1 mm;Φ: 6.35,7.48,9.53 mm;f: 0.0333–1 mm/rev;V_c: 6,7.5,9 m/min; Coating: without.
Brad & Spur Drill [25] 		t: 2–3 mm;f: 0.006–0.07$\frac{mm}{rev}$;V_c: 120 m/min
	Veniali et al. [25]	t: 3 mm;Φ: 3–8 mm;f: 0.026–0.094 mm/rev;V_c: 60–120 m/min; Coating: without.
	Bhattacharyya et al. [26]	t: 6 mm;Φ: 10 mm;f: 0.1 mm/rev;V_c: 30 m/min; Coating: without.
Tube Drill [23] 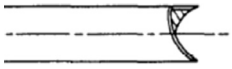	Bishop et al. [23]	t: 4 mm;Φ: 9.5 mm;f: 0.05 mm/rev;V_c: 22.3,40.4 m/min; Coating: without.
Core Drill [20] 	Zheng et al. [20]	t: 6–14 mm; Φ: 24 mm;V_c: 96–241 m/min; Coating: diamond.
Saw Drill [21] 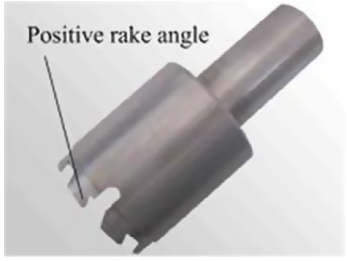	Gao et al. [21]	t: 2 mm;Φ: 30 mm;f: 5x10–4 mm/rev;V_c: 943 m/min; Coating: diamond.

Table 2
Mechanical properties for the aramid material.

Properties	Aramid
E1 (MPa)	18,000
E2 (MPa)	18,000
E3 (MPa)	6000
υ12	0.25
υ13	0.33
υ23	0.33
G12 (MPa)	770
G13 (MPa)	2600
G23 (MPa)	2600

3. Results and discussion

In this section, drilling performance is analyzed in terms of thrust force, torque and damage extension.

3.1. Thrust force and torque evolution

Thrust force and torque evolution were recorded during each test (all conditions were tested three times obtaining variations with respect to the mean value smaller than 4%, represented and analyzed results correspond to the mean values). The evolution of these variables during the drill entrance is shown in Fig. 4 for the case corresponding to

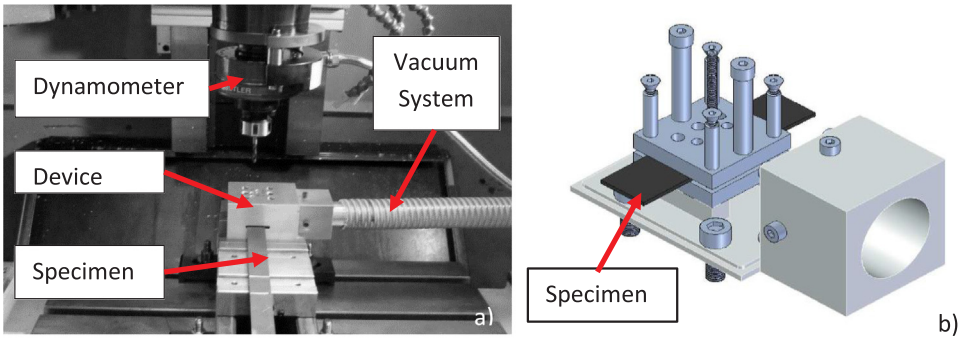

Fig. 1. a) Machining center used for drilling tests, showing Dynamometer Kistler 9123C, vacuum system for chip collection and special device. b) special device detail.

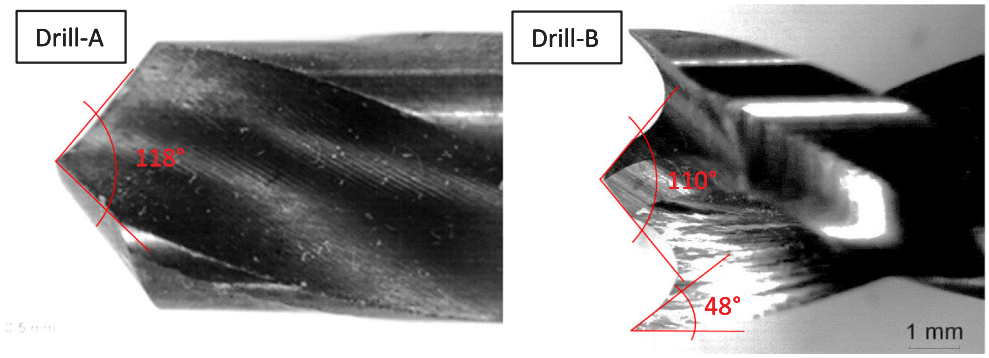

Fig. 2. Drill-A: Twist HSS drill (118°) and Drill-B: Brad & Spur HSS drill (110°).

Table 3
Cutting parameters used in drilling tests.

Drill A: Twist HSS drill	Case	V_c [m/min]	Feed [mm/rev]	Drill B: Brad & Spur HSS drill	Case	V_c [m/min]	Feed [mm/rev]
	1	23	0.025		16	23	0.025
	2		0.05		17		0.05
	3		0.1		18		0.1
	4	40	0.025		19	40	0.025
	5		0.05		20		0.05
	6		0.1		21		0.1
	7	57	0.025		22	57	0.025
	8		0.05		23		0.05
	9		0.1		24		0.1
	10	75	0.025		25	75	0.025
	11		0.05		26		0.05
	12		0.1		27		0.1
	13	92	0.025		28	92	0.025
	14		0.05		29		0.05
	15		0.1		30		0.1

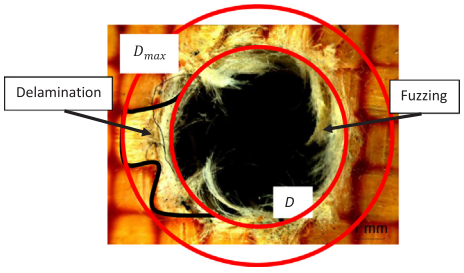

Fig. 3. Damaged measurement in the composite.

V = 110 m/min and f = 0.1 mm/rev. For the twist drill, maximum values of the thrust force were obtained when all the conical part shape of the drill was entered the thickness of the sample and the tip of the tool has not reached the bottom surface of the sample (see Fig. 4.a)). For depths corresponding to intermediate position B-C) the cross section of the undeformed chip is maximum and also the stiffness of the sample is elevated since a significant number of layers remain uncut. On the other hand, the maximum values of the torque were recorded for the position in which the tip of the tool was facing the sample bottom and the whole conical zone was out of the laminate (see Fig. 4.a), points between C-D), this effect is related to the friction force due to the uncut Kevlar fibers (fuzzing) added to cutting torque. Similar behavior has been observed for the rest of conditions analysed.

For the Brad & Spur drill, maximum values of the thrust force were obtained when the outer edges of the drill are cutting the last layers and the tip of the tool is outside the material (see Fig. 4.b)). At the intermediate points (C-E), and when the tip of the tool approaches the last layers of the sample, there is a reduction in the thrust force related to the decrease in the strength of the material, as few layers remain uncut. Once the tip of the drill has come out, the force increases due to the action of the outer edges. On the other hand, the maximum values of the torque for the Brad & Spur drill was found for the position in which the whole cutting area of the drill was out of the sample, being related to the friction between the uncut yarns (fuzzing) and the drill body.

During the tests, the effect of the feed and the cutting speed on the thrust force and torque was studied. Maximum values of the thrust force and torque obtained for each test are presented in Fig. 5. In general, for the twist drill, thrust force slightly decreases with cutting speed for the cases with largest feed, however, for the smallest feed thrust forces seems independent of the cutting speed (see Fig. 5.a)), this contrast with the results found by other researcher in glass fiber specimens [32], where the effect of the cutting speed can be neglected. In case of the Brad & Spur drill, no clear trend is observed, although is remarkable de fact that for the largest cutting speed are obtained the smallest thrust forces (see Fig. 5.b)), this effect was not found by other author under similar conditions [25].The effect of the cutting speed for both tools on the torque is not so similar (see Fig. 5.c) and Fig. 5.d)). As was highlighted in the study of Veniali et al. [25], for the Brad & Spur drill no clear tendency can be observed, however, for the Twist drill the tendency lines show a clear decrement in the torque with the increment of the cutting speeds. On the other hand, since the cross section of the chip increases with the feed, the thrust force and torque increased with the feed.

3.2. Damage

3.2.1. Damage evolution

Experimental observations reflect similarities with the results reported by Veniali et al. [25] (Fig. 6). The influence of feed on the damage found in the sample is lower for Twist drill, than in the case of Brad & Spur drill.

However, the effect that the feed has on the damage for both exit and entry side is different for each tool. Therefore, in general, increments in feed result in a decrease in the damage generated during drilling for the Twist drill, this effect is in disagreement with the result obtained by Sinan Liu et al. [28], where, as the feed was increased, the delamination was increased, however, the feed rates used in this work are much larger and it may help to break the fiber before the debonding of the layers. In the case of the Brad & Spur drill the opposite effect is observed, this is in agreement with the results found in the literature [25]. The cutting speed affect to the damage found on the entry and exit side of the sample in a similar way for both drill geometries. Thus, for higher cutting speed are obtained lower damages, being the largest variations those obtained for the Brad & Spur drill, these results make sense, as the cutting speed is increased, the resultants of the deformation of the fiber on the bonding plane between layer are higher, so less force in the plane perpendicular to the bonding plane are originated,

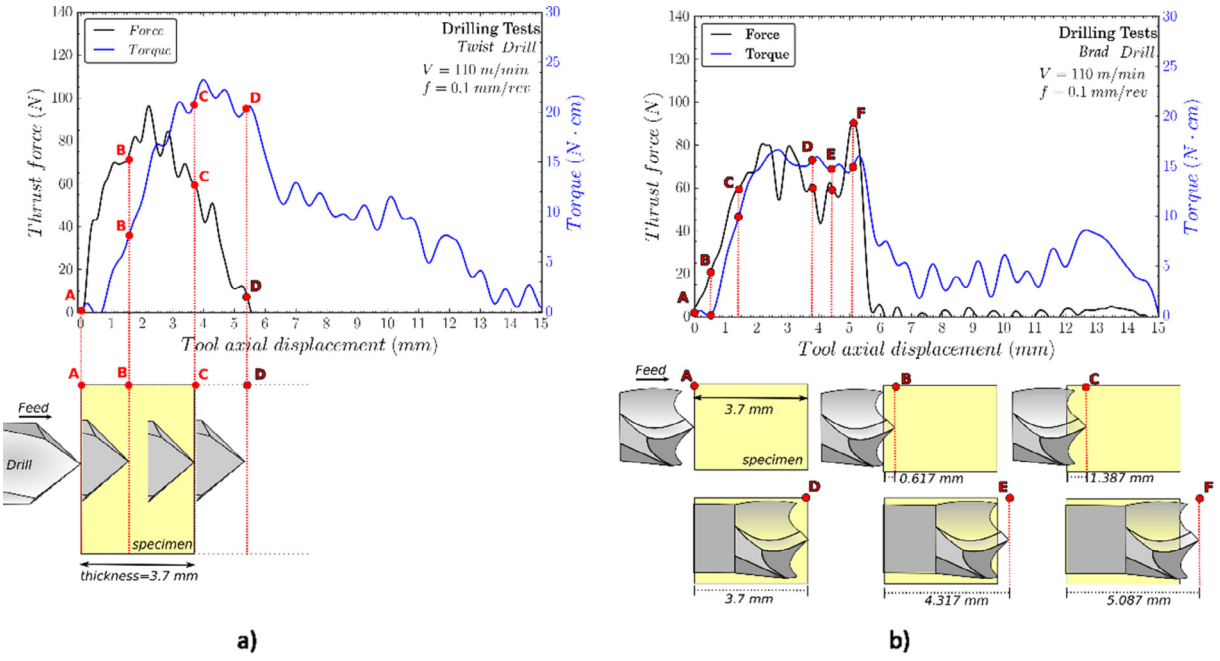

Fig. 4. Evolution of the Thrust force and Torque with the drill movement: a) Twist drill and b) Brad &Spur drill.

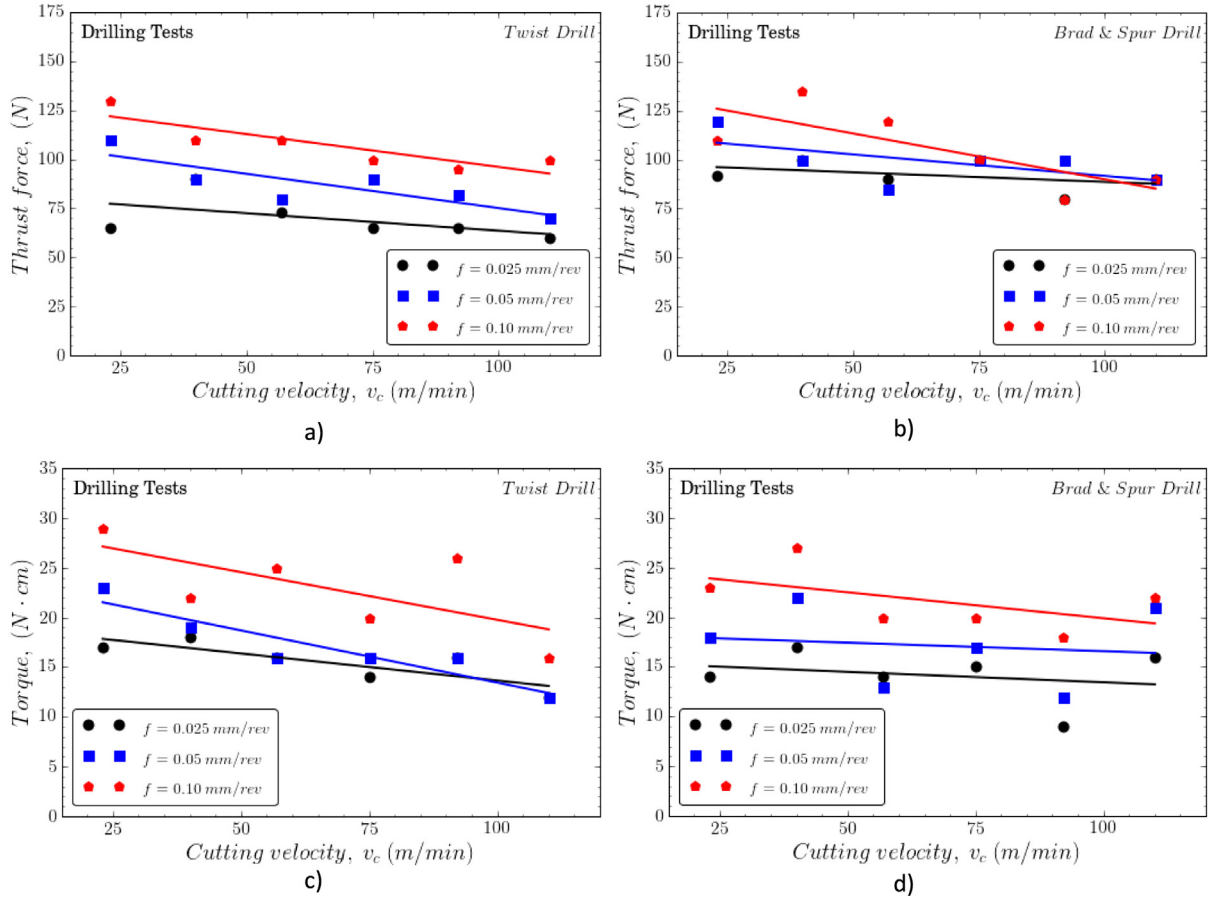

Fig. 5. a) Twist drill thrust force in function of the cutting speed at three different feeds. b) Brad & Spur drill thrust force in function of the cutting speed at three different feeds. c) Twist drill torque in function of the cutting speed at three different feeds. b) Brad & Spur drill torque in function of the cutting speed at three different feeds.

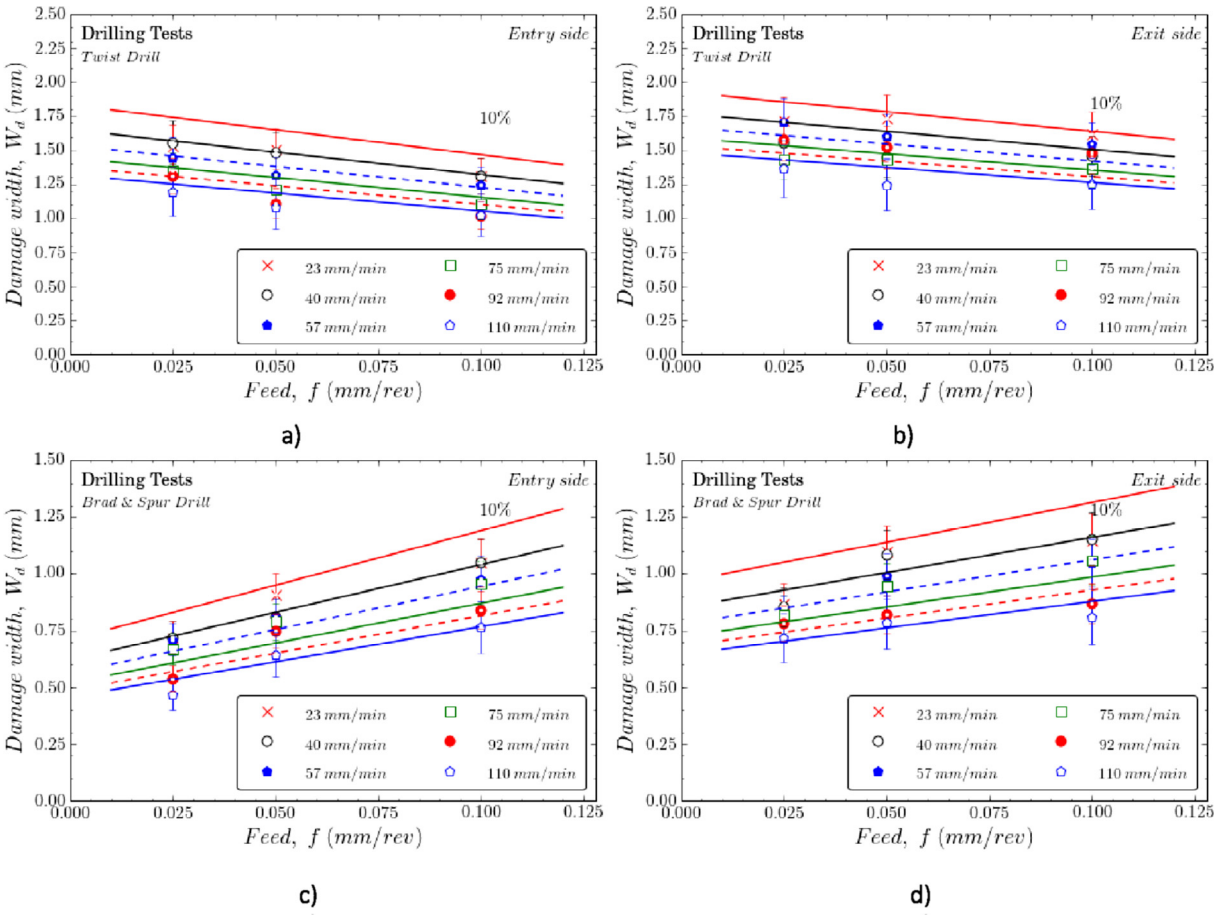

Fig. 6. Damage found on the entry and exit side for the Twist drill, a) and b) respectively. Damage found on the entry and exit side for the Brad & Spur drill, c) and d) respectively.

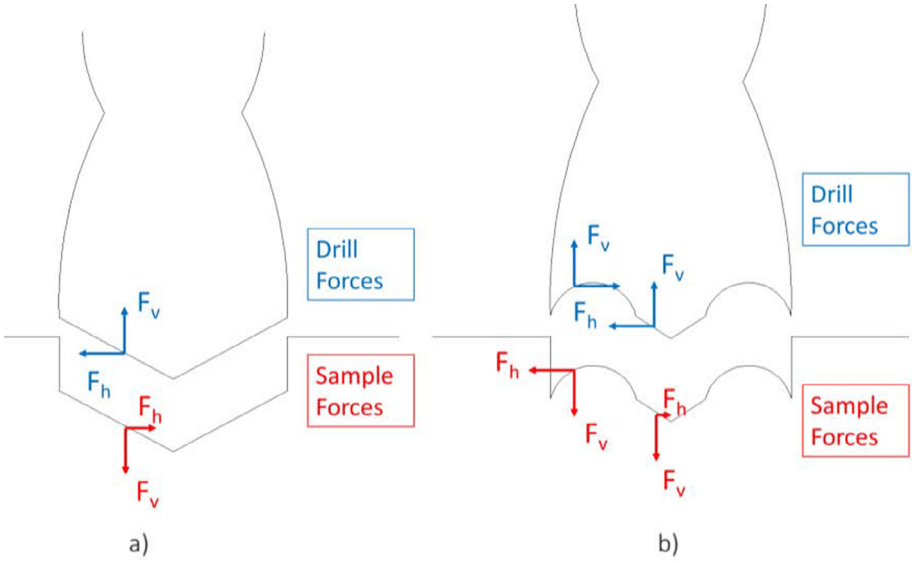

Fig. 7. Resultant forces on the sample and on the drills, a) Twist drill and b) Brad & Spur drill.

hence less fiber are pushing out or peeling up the layers.

Tests show that for equivalent conditions, the tool with a pure positive angle produces larger damages on both sides of the sample. This effect was previously explained attending to the cutting forces resultant of the cutting process [23]. In Fig. 7 are sketched the geometries of the used tools and the forces that act on the tool and on the sample. The resultant forces that the tool applies on the holes (see Fig. 7, blue color) show how in the case of the Twist drill the forces push the material outwards while for Brad & Spur drill the forces push the material inwards. Resultant forces pushing the material outwards favor the damage of the sample.

Regarding the fuzzing defect, in general it was found better results

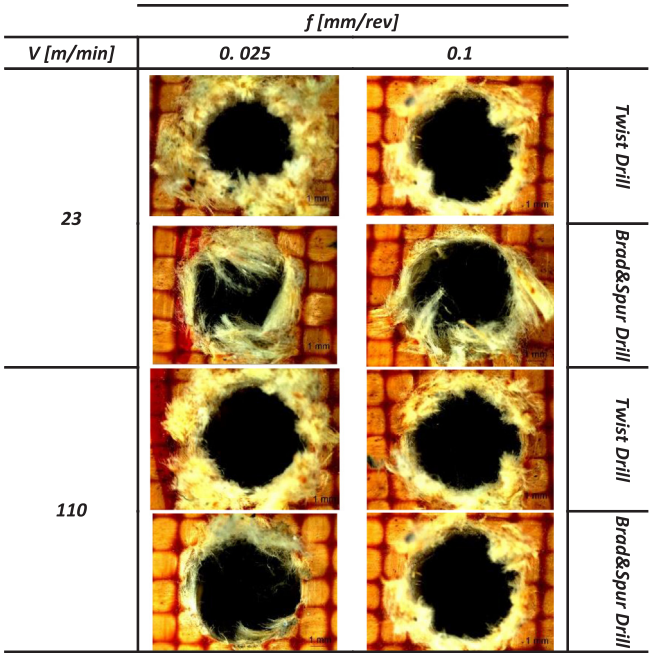

Fig. 8. Fuzzing found under different cutting conditions.

Fig. 9. Drills after performing a hole at a cutting speed of 23 m/min and a feed of 0.025 mm/rev; a) Brad & Spur and b) Twist respectively.

Table 4
Constants values obtained for the empirical model.

	Twist Drill			Brad & Spur Drill		
	A_1 (rev)	A_2 (mm)	A_3 (−)	A_1 (rev)	A_2 (mm)	A_3 (−)
Entry side	−3.3	1.65	0.2	4.2	0.62	0.26
Exit side	−2.65	1.77	0.16	3.1	0.85	0.24

with the use of the Brad & Spur geometry. In Fig. 8 is shown the fuzzing for both tools for feeds of 0.025 and 0.1 mm/rev and for two cutting speeds 23 and 110 m/min. The effect of the cutting parameters on the fuzzing was qualitatively analyzed. For the Twist geometry, was

Table 5
Constant values for Veniali et al. model found for the studied process.

	Twist Drill		Brad & Spur Drill	
	B_1 (N^{-1}mm)	B_2 (mm)	B_1 (N^{-1}mm)	B_2 (mm)
Entry side	0.0003	1.241	0.0075	0.039
Exit side	0.0016	1.348	0.0072	0.202

observed a better behavior in term of the fuzzing defect when lower speeds and high feeds were used, this result was also found in the literature [28] . In case of the Brad & Spur geometry, the effect of the cutting parameters on the fuzzing was the opposite, being obtained the best results in term of the fuzzing for higher cutting speeds and lower feeds.

It can be observed in Fig. 8, how different are the type of fiber breakages in function of the type of tool geometry used in each tests. In case of the Twist geometry, it is found that a lot of fibers get disposed forming a mess around the hole, however, this disposition of the fibers around the hole is not found in case of the Brad & Spur geometry, where it seems that the uncut fibers are clearly oriented with the direction of the tool rotation. The explanation of this effect comes from the tendency that has the fibers to be wrapped around the drill in case of using the Brad & Spur geometry. This effect decreases as the cutting speed and feed increase. In Fig. 9.a) is shown the state of a Brad & Spur drill after performing a hole at a cutting speed of 23 m/min and a feed of 0.025 mm/rev, whereas in Fig. 9.b) can be appreciated none fiber around a Twist drill for the same cutting conditions.

Due to the phenome explained in the paragraph above, it can be also explained another factor that makes the hole seems to have a better quality in term of the damage area for the Brad & Spur tool. Since the mechanism of fiber breakage may be slightly different for both geometries, appearing for the case of the Brad & Spur geometry a new source of tension for the fibers, which comes for the fact that the fiber get pull from the material by the wrapping action of the tool.

3.2.2. Damage prediction

The prediction of hole quality is carried out in terms of the damage parameter W_d. An empirical model proposed in Veniali et al. [25] has been used to predict damage parameter related to cutting parameters:

$$W_d(f) = A_1 * f + A_2 \tag{2}$$

Where A_1 and A_2 are material-dependent constants to be determined. From the previous equation, a new term has been added in this work in order to account for the effect of cutting speed $\left[1 - A_3 * ln\left(\frac{V_i}{V_0}\right)\right]$:

$$W_d(f) = A_1 * f + A_2 \cdot \left[1 - A_3 * ln\left(\frac{V_i}{V_0}\right)\right] \tag{3}$$

Where A_3 is the cutting velocity material constant. V_i and V_0 are the cutting velocity of the test and the reference cutting velocity, stated equal to the velocity tested of $V_0 = 40$ m/min. These parameters are evaluated from experimental data.

Fig. 6 shows good correlation between model predictions and the damage found though the experiments for both drills analysed. Note that the error is lower than 10% for all cases. The values obtained are summarized in Table 4.

Finally, the expressions for entry and exit damage are:

$$\text{Twist Drill} \begin{cases} W_d(f) = -3.30 * f + 1.65 \cdot \left[1 - 0.2 * ln\left(\frac{V_i}{40}\right)\right] & \textit{for entry side} \\ W_d(f) = -2.65 * f + 1.77 \cdot \left[1 - 0.16 * ln\left(\frac{V_i}{40}\right)\right] & \textit{for exit side} \end{cases} \tag{4a}$$

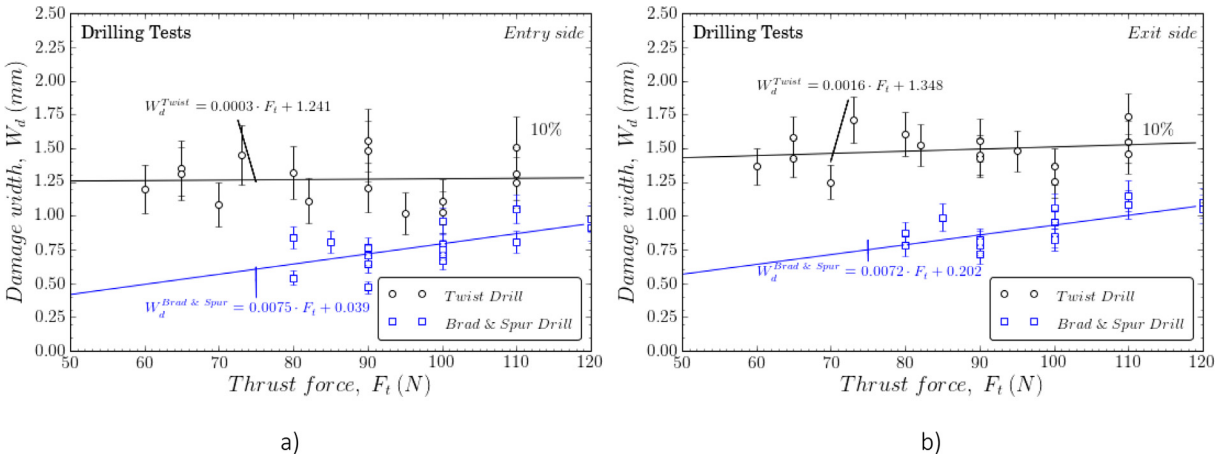

Fig. 10. Correlation between the delamination found in the experiments on the entry and exit side of the sample with respect the predicted values, a) and b) respectively.

Brad & *Spur Drill*

$$\begin{cases} W_d(f) = 4.2{*}f + 0.62{\cdot}\left[1{-}0.26{*}ln\left(\frac{V_i}{40}\right)\right] & for\ entry\ side \\ W_d(f) = 3.1{*}f + 0.85{\cdot}\left[1{-}0.24{*}ln\left(\frac{V_i}{40}\right)\right] & for\ exit\ side \end{cases} \quad (4b)$$

Moreover, the damage parameter has been related to the thrust force F_t through the relation proposed by Veniali et al. [25], where B_1 and B_2 are constants.

$$W_d(F_t) = B_1{*}F_t + B_2 \quad (5)$$

The constant values obtained from the experiments are presented in the Table 5, obtaining the Eqs. (6a) and (6b).

$$\text{Twist Drill}\begin{cases} W_d(F_t) = 0.0003{\cdot}F_t + 1.241 & for\ entry\ side \\ W_d(F_t) = 0.0016{\cdot}F_t + 1.348 & for\ exit\ side \end{cases} \quad (6a)$$

$$\text{Brad \& } SpurDrill\begin{cases} W_d(F_t) = 0.0075{\cdot}F_t + 0.039 & for\ entry\ side \\ W_d(F_t) = 0.0072{*}F_t + 0.202 & for\ exit\ side \end{cases} \quad (6b)$$

The model shows good correlation with the experimental data (see Fig. 10). The thrust force presents higher effect on the damage parameter at the entry side for the Brad & Spur geometry, while it has similar effect for both tools in the damage at the exit side. Similar tendencies were obtained by Veniali et al. [25] for the Brad & Spur tool.

4. Conclusion

In this work, an experimental and analytical analysis of drilling process of aramid composite using two tool geometries has been performed. Fuzzing was the dominant induced damage, being also found delamination in most of cases.

The comparison between the tested drills showed, in general, lower values of thrust force for the Twist drill particularly when low feed and high cutting velocities were chosen. However, the torque was similar for both tools.

For the tested conditions, lower values of delamination at the entry and exit side were found for the Brad & Spur drill. For the Twist drill it was observed better behavior in terms of the delamination found at the entry and exit side when large feeds and cutting speeds were selected. However, in case of the Brad & Spur drill, better results in term of delamination found at the entry and exit were obtained for higher speed and lower feed, being the effect of the feed on the delamination the opposite to the one found for the twist drill.

Regarding fuzzing defect, the Brad & Spur geometry showed better performance than the Twist geometry. In case of the Twist geometry, it was observed a better behavior when lower speeds and high feeds were use. In case of the Brad & Spur geometry, the effect of the cutting parameters was the opposite, being obtained the best results in term of the fuzzing for higher cutting speeds and lower feeds.

In general, for the range of cutting parameters tested in this study, a better behavior was found for the Brad & Spur drill, being the best combination to avoid delamination and fuzzing, the lowest feed and the highest cutting speed.

Mechanistic model was developed in order to predict the damage factor accounting for the effect of the cutting speed, the feed and the thrust force. The model showed good correlation with the experiments being an interesting tool to be implemented in industrial environment.

Acknowledgments

The authors are indebted to the Spanish company FECSA for providing the material tested in the paper.

The authors acknowledge the Ministry of Economy and Competitiveness of Spain and FEDER program under the Projects: RTC-2015-3887-8, DPI2017-88166-R and DPI2017-89197-C2-1-R for the financial support of the work.

References

[1] Galvez P, Quesada A, Martinez MA, Abenojar J, Boada MJL, Diaz V. Study of the behaviour of adhesive joints of steel with CFRP for its application in bus structures. Compos Part B Eng 2017;129:41–6. http://dx.doi.org/10.1016/j.compositesb.2017.07.018.

[2] Olmedo A, Santiuste C, Barbero E. An analytical model for predicting the stiffness and strength of pinned-joint composite laminates. Compos Sci Technol 2014;90:67–73. http://dx.doi.org/10.1016/j.compscitech.2013.10.014.

[3] Fernández-Pérez J, Cantero JL, Díaz-Álvarez J, Miguélez MH. Influence of cutting parameters on tool wear and hole quality in composite aerospace components drilling. Compos Struct 2017;178. http://dx.doi.org/10.1016/j.compstruct.2017.06.043.

[4] Simpson B, Dicken PJ. Integration of machining and inspection in aerospace manufacturing. IOP Conf Ser Mater Sci Eng 2011;26. http://dx.doi.org/10.1088/1757-899X/26/1/012014.

[5] Herbert MA, Shetty D, Shetty R, Shivamurthy B. Effect of process parameters on delamination, thrust force and torque in drilling of carbon fiber epoxy composite. Res J Recent Sci 2013;2:47–51.

[6] Kumar D, Sing KK. Experimental analysis of Delamination, Thrust Force and Surface roughness on Drilling of Glass Fibre Reinforced Polymer Composites Material Using Different Drills. Mater Today Proc 2017;4:7618–27. http://dx.doi.org/10.1016/j.matpr.2017.07.095.

[7] Feito N, Díaz-Álvarez J, López-Puente J, Miguelez MH. Experimental and numerical analysis of step drill bit performance when drilling woven CFRPs. Compos Struct 2017. http://dx.doi.org/10.1016/j.compstruct.2017.10.061.

[8] Davim JP, Rubio JC, Abrao AM. A novel approach based on digital image analysis to evaluate the delamination factor after drilling composite laminates. Compos Sci Technol 2007;67:1939–45. http://dx.doi.org/10.1016/j.compscitech.2006.10.009.

[9] Feito N, Díaz-Álvarez J, Díaz-Álvarez A, Cantero JL, Miguélez MH. Experimental analysis of the influence of drill point angle and wear on the drilling of woven CFRPs. Materials (Basel) 2014;7:4258–71. http://dx.doi.org/10.3390/ma7064258.

[10] Lissek F, Tegas J, Kaufeld M. Damage quantification for the machining of CFRP : An introduction about characteristic values considering shape and orientation of drilling-induced delamination. Procedia Eng 2016;149:2–16. http://dx.doi.org/10.1016/j.proeng.2016.06.632.

[11] Liu DF, Tang YJ, Cong WL. A review of mechanical drilling for composite laminates. Compos Struct 2012;94:1265–79. http://dx.doi.org/10.1016/j.compstruct.2011.11.024.

[12] Jia Z, Fu R, Niu B, Qian B, Bai Y, Wang F. Novel drill structure for damage reduction in drilling CFRP composites. Int J Mach Tools Manuf 2016;110:55–65. http://dx.doi.org/10.1016/j.ijmachtools.2016.08.006.

[13] Akbari N, Youse J, Ahmadi M, Minak G, Hosseini-toudeshky H, Sheibanian F. Static strength and damage evaluation of high speed drilled composite material using acoustic emission and fi nite element techniques. Eng Fract Mech 2018. http://dx.doi.org/10.1016/j.engfracmech.2018.04.020.

[14] Díaz-Álvarez A, Rubio-López Á, Santiuste C, Miguélez MH. Experimental analysis of drilling induced damage in biocomposites. Text Res J 2017. http://dx.doi.org/10.1177/0040517517725118. 004051751772511.

[15] Bajpai PK, Debnath K, Singh I. Hole making in natural fiber-reinforced polylactic acid laminates. J Thermoplast Compos Mater 2017;30:30–46. http://dx.doi.org/10.1177/0892705715575094.

[16] Isa MT, Ahmed AS, Aderemi BO, Taib RM, Mohammed-Dabo IA. Effect of fiber type and combinations on the mechanical, physical and thermal stability properties of polyester hybrid composites. Compos Part B Eng 2013;52:217–23. http://dx.doi.org/10.1016/j.compositesb.2013.04.018.

[17] Chouhan H, Singh D, Parmar V, Kalyanasundaram D, Bhatnagar N. Laser machining of Kevlar fiber reinforced laminates – Effect of polyetherimide versus polypropylene matrix. Compos Sci Technol 2016;134:267–74. http://dx.doi.org/10.1016/j.compscitech.2016.08.026.

[18] Dixit D, Pal R, Kapoor G, Stabenau M. 6 – Lightweight composite materials processing Elsevier Ltd; 2016. doi:10.1016/B978-0-08-100406-7.00006-4.

[19] Jie L. The formation and effect of interlayer gap in dry drilling of stacked metal materials. Int J Adv Manuf Technol 2013;69:1263–72. http://dx.doi.org/10.1007/s00170-013-5112-9.

[20] Zheng L, Zhou H, Gao C, Yuan J. Hole drilling in ceramics/Kevlar fiber reinforced plastics double-plate composite armor using diamond core drill. Mater Des 2012;40:461–6. http://dx.doi.org/10.1016/j.matdes.2012.04.011.

[21] Gao H, Zhuang Y, Wang B, Huang JL. Study on the Combined Machining Technology of Sawing and Grinding for Drilling Aramid/Epoxy Composites. Adv Mater Res 2012;565:436–41. http://dx.doi.org/10.4028/www.scientific.net/AMR.565.436.

[22] Wu LF, Zhu JG, Xie HM. Investigation of residual stress in 2D plane weave aramid fibre composite plates using moiré interferometry and hole-drilling technique. Strain 2015;51:429–43. http://dx.doi.org/10.1111/str.12155.

[23] Bishop GR, Gindy NNZ. An investigation into the drilling of ballistic Kevlar composites. Compos Manuf 1990;1:155–9. http://dx.doi.org/10.1016/0956-7143(90)90162-P.

[24] Di Ilio A, Tagliaferri V, Veniali F. Cutting mechanisms in drilling of aramid composites. Int J Mach Tools Manuf 1991;31:155–65. http://dx.doi.org/10.1016/0890-6955(91)90001-J.

[25] Veniali F, Di Illio A, Tagliaferri V. An experimental study of the drilling of aramid composites. J Energy Resour Technol 1995;117:271–8.

[26] Bhattacharyya D, Horrigan DPW. A study of hole drilling in Kevlar composites. Compos Sci Technol 1998;58:267–83. http://dx.doi.org/10.1016/S0266-3538(97)00127-9.

[27] Shuaib AN, Al-Sulaiman FA, Hamid F. Machinability of Kevlar 49 composite laminates while using standard TiN coated HSS drills. Mach Sci Technol 2004;8:449–67. http://dx.doi.org/10.1081/LMST-200041116.

[28] Liu S, Yang T, Liu C, Du Y, Gong W. Investigation of hole quality during drilling of KFRP based on the interaction between collars and cutter. Int J Adv Manuf Technol 2018;95:4101–16. http://dx.doi.org/10.1007/s00170-017-1520-6.

[29] Shyha IS, Aspinwall DK, Soo SL, Bradley S. International Journal of Machine Tools & Manufacture Drill geometry and operating effects when cutting small diameter holes in CFRP. Int J Mach Tools Manuf 2009;49:1008–14. http://dx.doi.org/10.1016/j.ijmachtools.2009.05.009.

[30] Mufarrih A, Soepangkat BOP, Krisnanto I. Multi Response Optimization Using Taguchi-Grey-Fuzzy Method in Drilling of Kevlar Fiber Reinforced Polymer (KFRP) Stacked. Appl Mech Mater 2016;836:179–84. http://dx.doi.org/10.4028/www.scientific.net/AMM.836.179.

[31] Won MS, Dharan CKH. Drilling of Aramid and Carbon Fiber Polymer Composites. J Manuf Sci Eng 2002;124:778. http://dx.doi.org/10.1115/1.1505854.

[32] Khashaba UA, Selmy AI, Megahed AA. Composites : Part A Machinability analysis in drilling woven GFR / epoxy composites : Part I - Effect of machining parameters. Compos Part A 2010;41:391–400. http://dx.doi.org/10.1016/j.compositesa.2009.11.006.